Enhanced conductivity in graphene layers and at their edges

S. Banerjee,[a)] M. Sardar, N. Gayathri, A. K. Tyagi, and Baldev Raj
Materials Science Division, Indira Gandhi Centre for Atomic Research, Kalpakkam 603102, T.N, India

(Received 25 May 2005; accepted 16 November 2005; published online 10 February 2006)

We have observed that the conductivity of graphene sheets is higher whenever they are loosely bound to the underlying bulk graphite. We also observe that certain edges of the graphene layers show sharp rise in current when biased, indicating enhanced electronic density of states spatially localized near those edges. In certain edges, we do not observe this phenomenon. These two observations, i.e., enhancement of conductivity of loosely bound layers and sharp rise in current at the edges are discussed with possible reasons and invoking recent theoretical predictions. © *2006 American Institute of Physics*. [DOI: 10.1063/1.2166697]

Various shaped nano-objects of carbon such as, single-walled and multiwalled nanotubes, fullerenes, nanocones, etc.,[1–4] are generally self-assembled by cutting and folding of graphene sheets depending on the growth conditions. Recently, electronic properties of these graphene nanostructures have attracted much attention from the point of view of basic research and applications.[5–11]

Highly oriented pyrolytic graphite (HOPG) is a periodical stack of two-dimensional (2D) graphene sheets (layers) along the c axis. Each sheet comprises hexagonal lattice of carbon bonded by strong σ bonding (sp^2) in the a-b plane [see Fig. 1(a)]. The perpendicular π-orbital electrons (along the c axis) are responsible for the conductivity along the a-b plane. The conduction occurs by the quantum mechanical hopping of these electrons. Each of these layers is weakly bonded to their neighboring layers by interlayer interaction forces. Because of the weak interlayer interaction forces, the graphene layers can easily slide against each other and peel off easily. It has been pointed out that graphene sheet edges strongly affect the π electronic states.[12] The edges of the graphene sheets are of two types: (1) armchair (cis) and (2) zigzag (trans) edges as shown in Fig. 1(b). It was theoretically shown that graphene sheets having zigzag edges possess edge states localized[8,12–20] at the zigzag edges. In contrast, armchair edges have no edge states at their edges, hence making the armchair edge less conducting than the zigzag edge.

The atomic force microscope (AFM) with conducting tip can be used to study the local electronic properties of conducting surfaces. We have used the AFM in contact mode with constant applied normal force on the tip. For the present investigation we have used freshly cleaved highly oriented pyrolytic graphite HOPG. By (simply) peeling off the surface layers using scotch tape, we were able to obtain steps and terraces with edges. The peeling off process dislocates the layers laterally and vertically. We have studied only monolayer steps to avoid complexity in the electrical analysis. Commercial AFM (NT-MDT, Russia) was used for the present investigation. Cantilevers used were platinum coated (CSG 10/Pt, NT-MDT) with radius of curvature of the tip ~35 nm and the cantilever elastic constant 0.1 N/m. For imaging in the contact mode the normal force between the surface and the tip was kept around ~25 nN (constant force mode). The sample was biased with 10–15 mV for measuring the local conductance (spreading resistance imaging) of the sample surface with the conducting tip. By measuring the tip-sample contact conductance (resistance) during the scanning process, we measure the local conductance of the sample surface. All the measurements were conducted at room temperature and ambient conditions. For topographic images we have only subtracted linear line fit along the scan direction from the scanned images and presented without any further filtration or averaging. For the conductance map we show only the raw data without any processing (processing the data was avoided as this can sometimes be misleading).

In Fig. 2(a) we show a topographic two-dimensional (2D) image of a selected region containing two monolayer steps/edges (staircase like) on the surface of the HOPG sample. In Fig. 2(b) we show the line profile of the line marked as A in Fig. 2(a). The sawtooth-like line profile is an artifact of the subtraction of a linear fit to the data to remove the tilt of the sample. We can clearly see the step heights to be around ~0.6 nm for the intermediate step (layer II) and ~0.7 nm for the top step (layer I), both values higher than the reported c-axis value of 0.35 nm for the HOPG sample. During the peeling-off process, the top few layers become loosely bonded to the sample surface resulting in the increased step heights.

In the inset of Fig. 3(a) we show conductance maps taken simultaneously along with topography [Fig. 2(a)] showing higher conductance (bright) for the top layer labeled as layer I. The intermediate (layer II) shows intermediate conductance (gray) and the lowest layer (layer III) shows the least conductance (dark). We also observe a bright current streak appearing on the top layer edge indicated by an arrow.

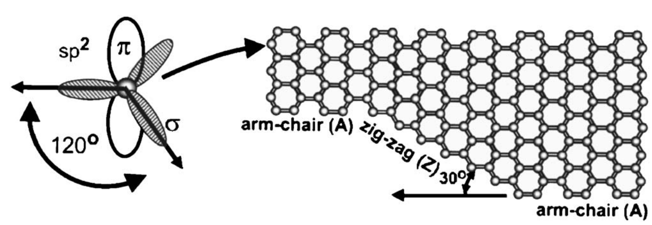

FIG. 1. (a) Carbon atoms showing sp^2 hybridized σ orbitals in the a-b plane and nonhybridized π orbitals along the c-axis of graphite layer. (b) Graphite sheet/ribbons showing armchair (cis) edge and zigzag (trans) edge obtained when cut at 30° with respect to each other.

[a)]On deputation from Surface Physics Division, Saha Institute of Nuclear Physics, 1/AF Bidhannagar, Kolkata, India; electronic mail: sangambanerjee@hotmail.com

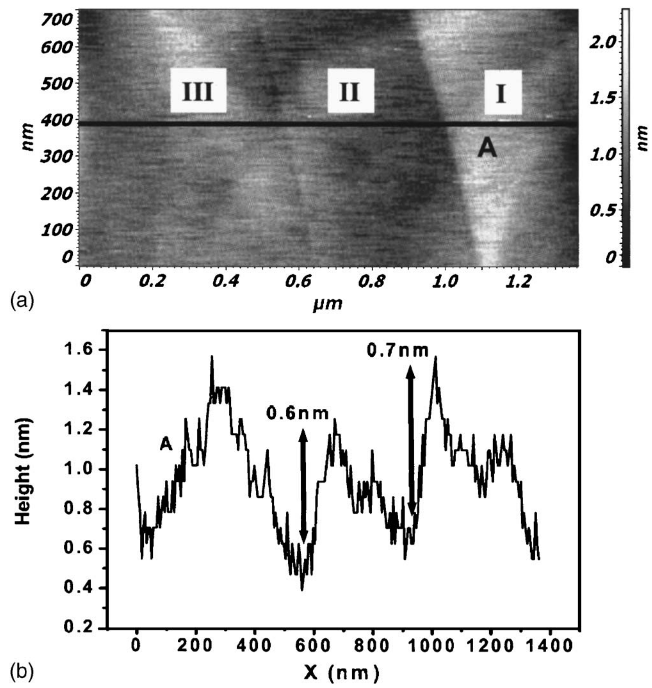

FIG. 2. (a) Topographic two-dimensional (2D) image of a selected region containing two monolayer steps/edges (staircase like) on the surface of the HOPG sample. (b) Two height profiles along the lines marked in (a) as A and B. The arrows indicate the step heights.

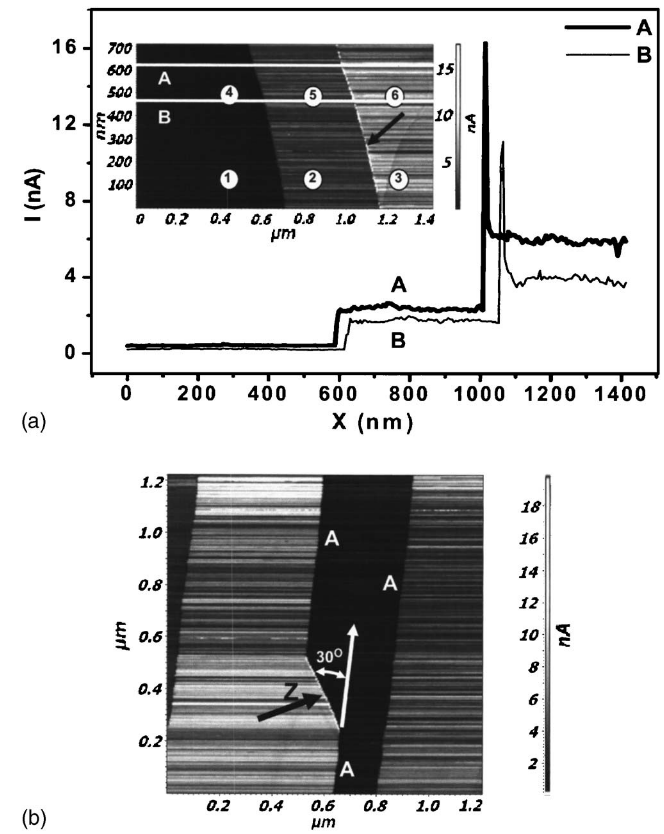

FIG. 3. (a) Line profiles of the conductance current of the lines marked A and B, respectively, in the inset. Inset: conductance map showing top layer having high conductance (bright-layer I), the intermediate step showing intermediate conductance (gray—layer II) and the lowest layer showing lowest conductance (dark—layer II). Bright current streaks appearing on certain edges are shown by an arrow. (b) Conductance map of a single ribbon edge containing two types of edges labeled A and Z. The angle between A and Z is 30° as schematically shown in Fig. 1(b). The edge labeled as Z (marked by arrow) shows bright current streak and the edge labeled as A does not show bright current streak at its edges.

The intermediate edge does not show this bright current streak on its edge. This observation clearly indicates the presence of two distinct types of edges on these two graphite layers. This is more illustrative in the line profile of the conductance current shown in Fig. 3(a) for the lines marked A and B in the inset. The current at the edges showing the bright streaks are 2–4 times the value measured on the terrace. In Fig. 3(b) we show a single ribbon edge containing two types of edges labeled as A and Z. The angle between A and Z is 30° as schematically shown in Fig. 1(b). The edge labeled as Z shows bright current streak and the edge labeled as A does not show this phenomenon.

We have also performed current-voltage (*I-V*) measurements as shown in Fig. 4 at various regions of steps (terraces) marked in Fig. 3(a). We clearly see that the layers which are brighter in the local conductance image show larger slope in the *I-V* measurement near zero bias. Combining topographic image, conductance map and *I-V* measurements, we find that the top layers which are dislodged more from the bulk have more conductivity. This is our main result.

During the peeling off process the top few layers of graphite peel off inhomogeneously forming a step-like structure as shown in Fig. 2. Vertical and lateral stresses are exerted on top layers causing them to dislocate vertically and laterally. It is known that π orbitals which are perpendicular to the graphite sheet are responsible for the electrical conductance along the sheet. It is also believed that the interlayer forces are the van der Waals' forces. We believe that the π electrons not only take part in conductivity, but also have to contribute substantially to the polarization cloud (without electron transfer) that gives the bonding between the layers. If the top layer is loosely bound, then the π electrons of the loosely bound top layers do not participate much in the bonding with the layer underneath. This makes the π electrons spread out more along the *a-b* plane causing an increase in the overlap of the orbitals along the *a-b* plane and thus leading to higher conductivity. Note: The carrier density does not change and it is only the orbital overlap which

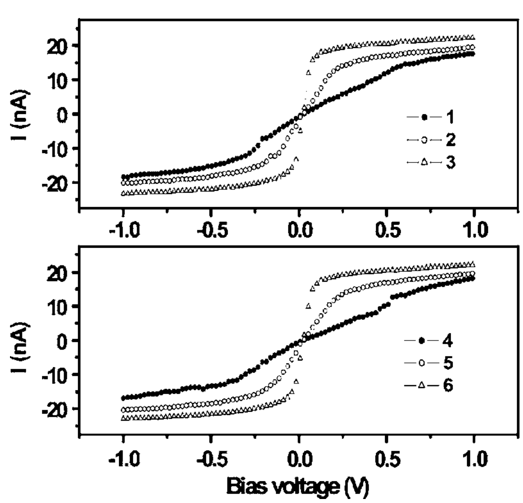

FIG. 4. Current-voltage (*I-V*) measurements at various regions of steps/terraces marked in the inset of Fig. 3(a). Low slope value in the *I-V* curve at zero-bias indicates lower conducting region than the region having higher slope.

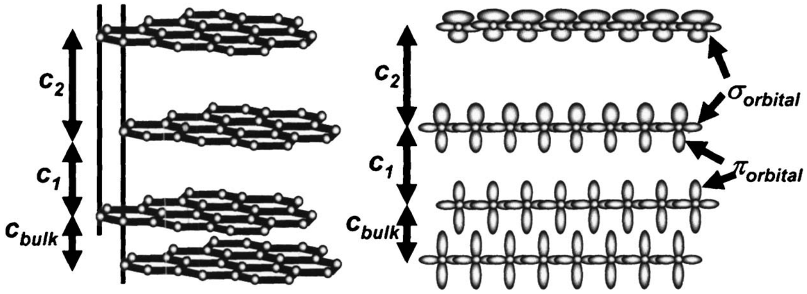

FIG. 5. Schematic representation of graphite layer separations $C_2 > C_1 > C_{\mathrm{bulk}}$. The top layer is loosely bound showing the π electrons/orbitals are spread out more along the *a-b* plane causing increase in the overlap of the orbitals leading to higher conductivity.

increases, thus leading to a higher conductivity.

The peeling of the layers was performed manually in an uncontrolled fashion. This can lead to different degrees of applied stress on different layers and cause different amounts of vertical displacement. The one which has a larger step height (*c*-axis distance) will be less bound (causing large orbital overlap along the plane) than the ribbon which has a lower step height (*c*-axis value). We motivate this schematically in Fig. 5. The difference in conductance among the steps can be explained invoking the argument that the loosely bound ribbons are more conducting than the tightly bound layers for the reasons given above.

Now, we will discuss the presence of sharp current peaks observed at the edges [inset of Fig. 3(a) and the Z region marked by arrow in Fig. 3(b)]. As mentioned earlier, there are mainly two types of edges formed on graphene sheets when it is cut (Fig. 1). Recently, detailed theoretical calculations have shown that zigzag edges have edge states localized at the edges having a higher electron density.[12–19] Hence these edges will have higher electrical conductance. Thus, during the mapping of the local conductance these edges will show up as brighter streaks. The layers can be oriented in a different direction with respect to each other and during the tearing process it will tear along any suitable (either zigzag or armchair) direction as we observe in Fig. 3(a). As mentioned earlier, the armchair edges have no electronic edge states and thus show no sharp peak in the current at its edges. Thus, we can say that the edges A are armchair edges and the edge Z is the zigzag edge in Fig. 3(b) [see Fig. 1(b) which shows the angle between the armchair and the zigzag is 30°].

To summarize, we have shown that when the graphene layers are strained and dislodged from the surface of the bulk graphite sample then the electrical conductivity of that layer enhances. The enhancement of the conductance depends on the degree of dislodgement of the layers. The larger the dislodgement of the layer the more enhanced is the electrical conductivity. The increase in the conductivity of these sheets can be explained only by assuming that the π electrons on the loosely bound sheets are not much involved in the binding between the layers and hence would have higher mobility (conductivity). We also observe a sharp increase or absence in conductance current at the edges of the graphite layers and this we have attributed to either zigzag shaped edges or armchair shaped edges, respectively. A more careful understanding of the stability of the edge states is surely needed so that one can imagine fabricating nano-patches bounded only by zigzag edges. These might support large orbital magnetic moment on the surface. The localized edge states may be one of the main causes of ferromagnetism in graphite.[21]

[1]For review see *Carbon Molecules and Materials*, edited by R. Setton, P. Bernier, and S. Lefrant (Taylor and Francis, New York, 2002).
[2]V. N. Popov, Mater. Sci. Eng., R. **43**, 61 (2004).
[3]S. P. Jordan and V. H. Crespi, Phys. Rev. Lett. **93**, 255504 (2004).
[4]R. Saito, G. Dresselhaus, and M. S. Dresselhaus, *Physical Properties of Carbon Nanotubes* (Imperial College Press, London, 1998).
[5]P. M. Ajayan and T. W. Ebbesen, Rep. Prog. Phys. **60**, 1025 (1997).
[6]S. P. Jordan and V. H. Crespi, Phys. Rev. Lett. **93**, 255504 (2004).
[7]I. L. Spain, in *Chemistry and Physics of Carbon*, edited by P. L. Walker and P. A. Thrower (Dekker, New York, 1981), Vol. 16.
[8]K. Wakabayashi, Phys. Rev. B **64**, 125428 (2001).
[9]J. C. Slonczewshi and P. R. Weiss, Phys. Rev. **109**, 272 (1958).
[10]J. W. McClure, Phys. Rev. **119**, 606 (1960).
[11]R. Setton, in *Carbon Molecules and Materials*, edited by R. Setton, P. Bernier, and S. Lefrant (Taylor and Francis, New York, 2002), p. 22.
[12]M. Fujita, K. Wakabayashi, K. Nakada, and K. Kusakabe, J. Phys. Soc. Jpn. **65**, 1920 (1996).
[13]K. Nakada, M. Fujita, G. Dresselhaus, and M. S. Dresselhaus, Phys. Rev. B **54**, 17954 (1996).
[14]K. Wakabayashi, M. Fujita, H. Ajiki, and M. Sigrist, Phys. Rev. B **59**, 8271 (1999).
[15]S. E. Stein and R. L. Brown, J. Am. Chem. Soc. **109**, 3721 (1987).
[16]H. Hosoya, Y.-D. Gao, K. Nakada, and M. Ohuchi, in *New Functionality Materials*, edited by C. T. Tsuruta, M. Doyama, and M. Sena (Elsevier, New York, 1993), p. 27.
[17]K. Tanaka, S. Yamashita, H. Yamabe, and T. Yamabe, Synth. Met. **17**, 143 (1987).
[18]M. Fujita, M. Yoshida, and K. Nakada, Fullerene Sci. Technol. **4**, 565 (1996).
[19]S. Ryu and Y. Hatsugai, Physica E (Amsterdam) **22**, 679 (2004).
[20]M. Elstner, D. Porezag, G. Jungnickel, J. Elsner, M. Haugk, T. Frauenheim, S. Suhai, and G. Seifert, Phys. Rev. B **58**, 7260 (1998).
[21]P. Esquinazi, A. Setzer, R. Hohne, C. Semmelhack, Y. Kopelevich, D. Spemann, T. Butz, B. Kohlstrunk, and M. Losche, Phys. Rev. B **66**, 024429 (2002).